IR, Raman and SERS spectra of 2-phenoxymethylbenzothiazole

C. Yohannan Panicker[a,*], Hema Tresa Varghese[b], Asha Raj[c], K. Raju[d], Tugba Ertan-Bolelli[e], Ilkay Yildiz[e], Ozlem Temiz-Arpaci[e], Carlos M. Granadeiro[f], Helena I.S. Nogueira[f]

[a] *Department of Physics, TKM College of Arts and Science, Kollam, Kerala, India*
[b] *Department of Physics, Fatima Mata National College, Kollam, Kerala, India*
[c] *Department of Physics, Government Polytechnic College, Attingal, Kerala, India*
[d] *Department of Physics, University College, Trivandrum, Kerala, India*
[e] *Ankara University, Faculty of Pharmacy, Department of Pharmaceutical Chemistry, Tandogan 06100, Ankara, Turkey*
[f] *Department of Chemistry, CICECO, University of Aveiro, 3810-193 Aveiro, Portugal*

ARTICLE INFO

ABSTRACT

The FT-IR and FT-Raman spectra of 2-phenoxymethylbenzothiazole were recorded and analyzed. The surface enhanced Raman scattering (SERS) spectrum was recorded in a silver colloid. The vibrational wavenumbers of the compound have been computed using the Hartree–Fock/6-31G* basis and compared with the experimental values. The appearance of the Ag–O stretching mode at 237 cm^{-1} in the SERS spectrum along with theoretically calculated atomic charge density, leads us to suggest that the molecule is adsorbed through the oxygen atom with the molecular plane tilted on the colloidal silver surface. The direction of charge transfer contribution to SERS has been discussed from the frontier orbital theory.

© 2009 Elsevier B.V. All rights reserved.

1. Introduction

Surface enhanced Raman scattering (SERS) spectroscopy is a well-established and highly effective technique of observing Raman scattering from species present at trace concentrations [1,2]. It is a useful tool in surface chemistry because of its high sensitivity and potential in providing useful information regarding metal–adsorbate interactions [3,4]. The compounds containing a thiazole ring have shown useful biological properties and have been developed as fungicides, herbicides, or plant growth regulators [5]. The biological importance of thiazole derivatives was emphasized during the period 1941–1945, when research on the structure of the antibiotic penicillin showed the presence of a thiazolidine ring in this important therapeutic agent [6]. The 2-aminobenzothiazole molecule is known for its local anaesthetic action and has numerous applications in human and veterinary medicine [7]. It is a metabolite of methabenzthiazuron [8] and is reported to form the main fraction of soil-bound residues [9]. Anthelmintics exert their chemotherapeutic effect by interfering with some biochemical or physiological processes essential for the survival of the parasite in the host [10]. Several substituted benzimidazoles and benzothiazoles [11–14] have been identified as potent authelmintic

drugs. Benzothiazoles constitute an important class of compounds with profound interest to medicinal/industrial chemists as compounds bearing the benzothiazolyl moiety. They exhibit diverse biological properties such as antitumour [15,16], antimicrobial [17], antiglutamate/antiparkinson [18], broad spectrum Ca^{2+} channel antagonist [19], inhibition of enzymes such as aldose reductase [20], monoamine oxidase [21], lipoxygenase [22], cyclooxygenase [23], acetylcholine esterase [24], thrombin [25], proteases [26], H^+–K^+ ATpase [27], carbonic anhydrase [28], HCV helicase [29], plant growth regulation [30] and have industrial applications such as antioxidants [31], and vulcanization accelerators [32]. 2-Phenoxymethyl benzothiazole [33,34] was resynthesized for evaluating its biological activity. This structure was found to be very potent either against Gram positive bacteria *Staphylococcus aureus* with a MIC value [34] of 3.12 μg/ml or as an eukaryotic Topoisomerase II inhibitor [35]. Even, 2-phenoxymethylbenzothiazole (IC_{50} value of 11.4 μM) was found to be more active than the reference drug etoposide (IC_{50} value of 21.8 μM). Considering the enormous biological importance, we present here the detailed experimental and theoretical normal Raman spectroscopy, SERS and FT-IR spectra of the title compound.

2. Experimental

The FT-IR spectrum (Fig. 1) was recorded on a Pye Unicam SP-1025 spectrometer with KBr pellets. Raman spectra (Figs. 2 and 3)

---

* Corresponding author.
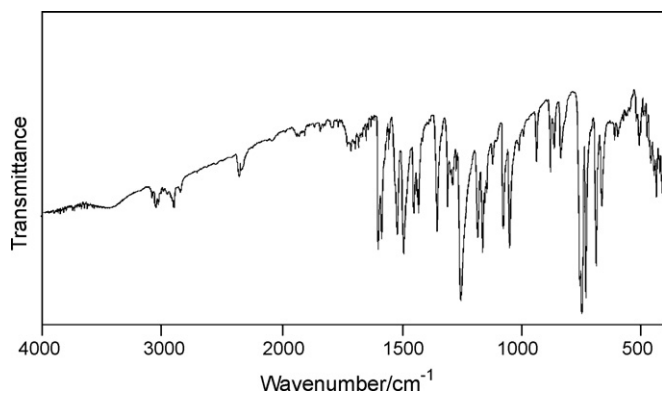 *E-mail address:* cyphyp@rediffmail.com (C.Y. Panicker).

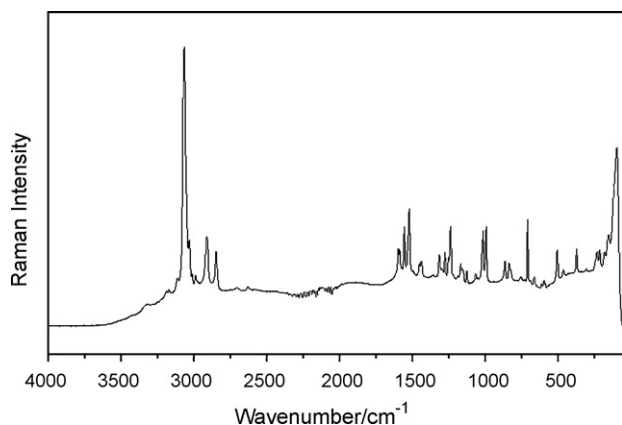**Fig. 1.** IR spectrum of 2-phenoxymethylbenzothiazole.

Fig. 2. Raman spectrum of 2-phenoxymethylbenzothiazole.

were recorded on a Bruker RFS 100/s FT instrument (Nd:YAG laser, 1064 nm excitation). The ^{1}H NMR spectra were obtained with a Bruker AC 80 MHz spectrometer and TMS was used as an internal standard. Elemental analysis was carried out with a Perkin-Elmer model 240-C apparatus. The results of the elemental analysis (C, H, N) were within ±0.4% of the calculated amounts. The aqueous silver colloid used in the SERS experiments was prepared by reduction of silver nitrate by sodium citrate, using the Lee–Meisel method [36,37]. Solutions of the compound were made up in ethanol (0.1 mmol in 1 cm^3 of solvent) and transferred by a microsyringe into the silver colloid (10 μl in 1 cm^3 of the colloid) such that the over all concentration was 10^{-3} mol dm^{-3}. Colloid aggregation

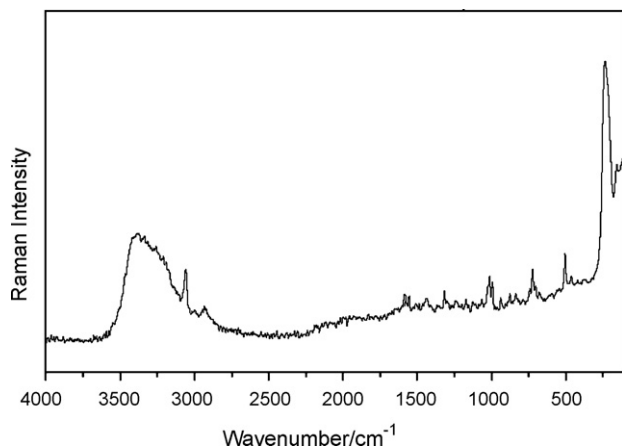**Fig. 3.** SERS spectrum of 2-phenoxymethylbenzothiazole.

was induced by addition of an aqueous solution of $MgCl_2$ (1 drop of a 2 mol dm^{-3} solution). Polyvinylpyrrolidone was then used to stabilize the colloid (1 drop of 0.1 g/10 cm^3 aqueous solution). The final colloid mixture was placed in a glass tube and the Raman spectrum was recorded.

3. Synthesis of 2-phenoxymethylbenzothiazole

The general synthetic procedure was employed to prepare the compound 2-phenoxymethylbenzothiazole involving the reaction of the phenoxyacetic acid with 2-aminothiophenol by refluxing in the presence of dehydrating agents in one step procedure. For the preparation of the title compound trimethylsilyl polyphosphate ester (PPSE) was used as the cyclodehydration reagent in the ring closure reactions [38].

A mixture of phenoxyacetic acid (5 mmol) and 2-aminothiophenol (6.9 mmol) was heated under reflux with stirring for 3 h at 140 °C in 15 ml PPSE. At the end of the reaction period, the mixture was taken to 30 ml dichloromethane and neutralized with 50 ml 1N NaOH solution. The organic layer was separated and the aqueous solution extracted with 3× 25 ml portions of CH_2Cl_2. The combined extracts were dried on Na_2SO_4, filtered and the solvent was removed with rotary evaporator. The residue was purified by flash chromatography, eluting with $CHCl_3$ and the obtained product was recrystallized using CH_2Cl_2/hexane. Yield 72%. Melting point 77–78 °C [34].

8.00–7.80 (m, 2H, C-5H(H9) and C-2H(H8)), 7.40–6.90 (m, 7H, C-6H(H10), C-1H(H7) and phenyl protons), 5.47 (s, 2H, CH_2 (C-14)).

4. Computational details

Calculations of the title compound were carried out with Gaussian03 program [39] using the HF/6-31G* basis set to predict the molecular structure and vibrational wavenumbers. Molecular geometry was fully optimized by Berny's optimization algorithm using redundant internal coordinates. Harmonic vibrational wavenumber values were calculated using the analytic second derivatives to confirm the convergence to minima on the potential surface. The wavenumber values computed at the Hartree–Fock level contain known systematic errors due to the negligence of electron correlation [40]. We therefore, have used the scaling factor value of 0.8929 for HF/6-31G* basis set. Parameters corresponding to optimized geometry of the title compound (Fig. 3) are given in Table 1. The absence of imaginary values of wavenumbers on the calculated vibrational spectrum confirms that the structure deduced corresponds to minimum energy. The assignment of the calculated wavenumbers is aided by the animation option of MOLEKEL program, which gives a visual presentation of the vibrational modes (Fig. 4) [41,42].

5. Results and discussion

5.1. IR and Raman spectra

The observed IR and Raman bands with their relative intensities, calculated values and assignments are given in Table 2. The C=N stretching skeletal bands [43–46] are observed in the range 1672–1566 cm^{-1}. Saxena et al. [44] reported a value 1608 cm^{-1} for polybenzodithiazole and Klots and Collier [47] reported a value of 1517 cm^{-1} for benzoxazole as υC=N stretching mode. Yang et al. [48] reported a band at 1626 cm^{-1} in the IR spectrum as υC=N for the oxazole ring. For the title compound, the HF calculations give υC=N mode at 1622 cm^{-1} and experimentally no bands are observed.

Table 1
Optimized geometrical parameters of 2-phenoxymethylbenzothiazole, atom labeling is according to Fig. 4.

Bond lengths (Å)		Bond angles (°)		Dihedral angles (°)	
C_1-C_2	1.3846	A(2,1,6)	120.9	D(6,1,2,8)	180.0
C_1-C_6	2.3972	A(2,1,7)	119.5	D(7,1,2,3)	−180.0
C_1-H_7	1.0727	A(6,1,7)	119.6	D(2,1,6,10)	−180.0
C_2-C_3	1.3851	A(1,2,3)	118.2	D(7,1,6,5)	180.0
C_2-H_8	1.0718	A(1,2,8)	120.7	D(1,2,3,11)	180.0
C_3-C_4	1.3921	A(3,2,8)	121.1	D(8,2,3,4)	−180.0
C_3-S_{11}	1.8095	A(2,3,4)	121.2	D(2,3,4,12)	−180.0
C_4-C_5	1.3888	A(2,3,11)	129.1	D(11,3,4,5)	−180.0
C_4-N_{12}	1.4011	A(4,3,11)	109.7	D(2,3,11,13)	180.0
C_5-C_6	1.3816	A(3,4,5)	120.4	D(3,4,5,9)	−180.0
C_5-H_9	1.0714	A(3,4,12)	114.9	D(12,4,5,6)	180.0
C_6-H_{10}	1.0724	A(5,4,12)	124.8	D(5,4,12,13)	−180.0
$S_{11}-C_{13}$	1.8181	A(4,5,6)	118.7	D(4,5,6,10)	−180.0
$N_{12}-C_{13}$	1.2704	A(4,5,9)	119.4	D(9,5,6,1)	180.0
$C_{13}-C_{14}$	1.4895	A(6,5,9)	121.9	D(3,11,13,14)	−180.0
$C_{14}-H_{15}$	1.0825	A(1,6,5)	120.7	D(4,12,13,14)	180.0
$C_{14}-H_{16}$	1.0825	A(1,6,10)	119.5	D(11,13,14,15)	−120.4
$C_{14}-O_{17}$	1.4307	A(5,6,10)	119.8	D(11,13,14,16)	120.4
$O_{17}-C_{18}$	1.3901	A(3,11,13)	86.7	D(12,13,14,15)	59.6
$C_{18}-C_{19}$	1.3846	A(4,12,13)	113.3	D(12,13,14,16)	−59.6
$C_{18}-C_{20}$	1.3846	A(11,13,12)	115.4	D(12,13,14,17)	180.0
$C_{19}-C_{21}$	1.3874	A(11,13,14)	121.5	D(13,14,17,18)	180.0
$C_{19}-H_{22}$	1.0721	A(12,13,14)	123.1	D(16,14,17,18)	−60.1
$C_{20}-C_{23}$	1.3874	A(13,14,15)	109.7	D(16,14,17,18)	60.1
$C_{20}-H_{24}$	1.0721	A(13,14,16)	109.7	D(14,17,18,19)	90.9
$C_{21}-C_{25}$	1.3884	A(13,14,17)	108.1	D(14,17,18,20)	−90.9
$C_{21}-H_{26}$	1.0727	A(15,14,16)	108.6	D(17,18,19,21)	178.6
$C_{23}-C_{25}$	1.3884	A(15,14,17)	110.4	D(17,18,19,22)	−0.4
$C_{23}-H_{27}$	1.0727	A(16,14,17)	110.4	D(20,18,19,21)	0.4
$C_{25}-H_{28}$	1.0726	A(14,17,18)	118.8	D(20,18,19,22)	−178.6
		A(17,18,19)	119.5	D(17,18,20,23)	−178.6
		A(17,18,20)	119.5	D(17,18,20,24)	0.4
		A(19,18,20)	121.0	D(19,18,20,23)	−0.4
		A(18,19,21)	119.3	D(19,18,20,24)	178.6
		A(18,19,22)	119.4	D(18,19,21,26)	−179.7
		A(21,19,22)	121.2	D(22,19,21,25)	178.9
		A(18,20,23)	119.3	D(22,19,21,26)	−0.8
		A(18,20,24)	119.4	D(18,20,23,27)	179.7
		A(23,20,24)	121.2	D(24,20,23,25)	−178.9
		A(19,21,25)	120.2	D(24,20,23,27)	0.8
		A(19,21,26)	119.7	D(19,21,25,23)	−0.3
		A(25,21,26)	120.1	D(19,21,25,28)	−179.9
		A(20,23,25)	120.2	D(26,21,25,23)	179.4
		A(20,23,27)	119.7	D(26,21,25,28)	−0.2
		A(25,23,27)	120.1	D(20,23,25,21)	0.3
		A(21,25,23)	119.8	D(20,23,25,28)	179.9
		A(21,25,28)	120.1	D(27,23,25,21)	−179.4
		A(23,25,28)	120.1	D(27,23,25,28)	0.2

The vibrations of the CH_2 group, the asymmetric stretch $\upsilon_{as}CH_2$, symmetric stretch υ_sCH_2, scissoring vibration δCH_2, appear in the region 2945 ± 45, 2885 ± 45 and 1445 ± 35 cm^{-1}, respectively [49,50]. The HF calculations give $\upsilon_{as}CH_2$ at 2920 cm^{-1} and υ_sCH_2 at 2873 cm^{-1}. The bands observed at 2905 cm^{-1} (IR), 2909 cm^{-1} (Raman) and 2840 cm^{-1} (IR), 2846 cm^{-1} (Raman) are assigned as asymmetric and symmetric CH_2 modes, respectively. In the present case, the band observed at 1497 cm^{-1} in the IR spectrum and
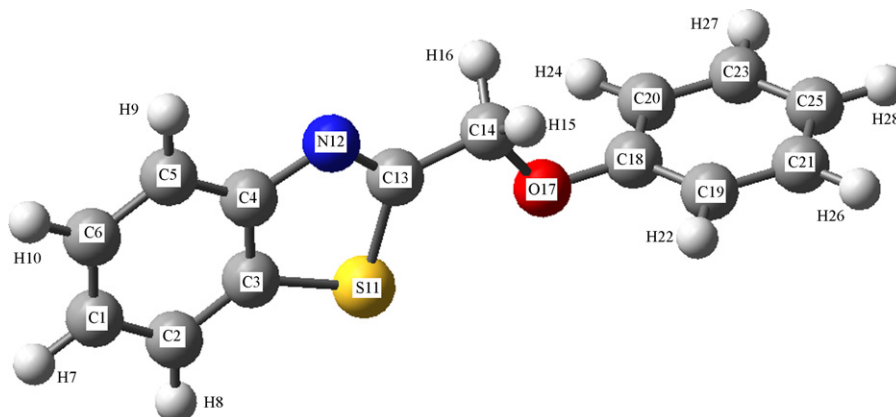
Fig. 4. Optimized geometry of 2-phenoxymethylbenzothiazole.

Table 2
Calculated vibrational wavenumbers, measured infrared and Raman bands positions and assignments of 2-phenoxymethylbenzothiazole.

$\upsilon_{(HF)}$ (cm^{-1})	$\upsilon_{(IR)}$ (cm^{-1})	$\upsilon_{(Raman)}$ (cm^{-1})	$\upsilon_{(HSERS)}$ (cm^{-1})	Assignments
3037	3088 w	3099 w	–	υCH II
3035	3052 w	3068 vvs	3060 s	υCH I
3031	–	3033 sh	–	υCH II
3029	3029 w	–		υCH I
3021	–	–		υCH I
3017	–	–		υCH II
3009	–	–		υCH I
3004	–	–		υCH II
2999	2985 w	2987 vw	2994 w	υCH I
2920	2905 w	2909 m	2935 wbr	υ_{as}CH$_2$
2873	2840 w	2846 m		υ_sCH$_2$
1622	–			υC=N
1612	–	–		υPh I
1599	1601 s	1588 m		υPh I
1594	1587 s	1586 sh		υPh II
1578	1559 w	1560 m	1575 w	υPh II
1497	1522 s	1523 s	1554 w	υPh I
1485	1497 s	–		δCH$_2$
1462	–	–		υPh II
1455	1454 m	1444 sh		υPh I
1452	1436 m	1436 w	1432 w	υPh II
1372	1357 s	1347 vw		ωCH$_2$
1326	1315 m	1315 w	1319 m	υPh I, CN
1289	1294 w	1276 w		δCH I
1245	1278 vw	1247 sh		υPh II
1230	1259 vvs	1238 m	1233 wbr	υC18–O17
1223	–	–		δCH II
1214	–	–		τCH$_2$
1169	1188 s	1177 vw	1172 w	δCH I
1163	1168 s	1168 w		υCC
1153	–	1153 sh		δCH II
1144	1140 w	–		δCH I
1118	1126 w	1126 w	1120 w	δCH II
1064	1079 s	1064 w	1066 w	δCH I
1053	1053 s	–		δCH II
1024	–	–		υC14–O17
1022	–	–		δCH I
1016	–	1016 m	1016 m	Ring breath II
1009	–	–		γCH II
1007	–	–		ρCH$_2$
1005	1000 w	–		Ring breath I
990	–	996 m	996 m	γCH I
960	–	–		γCH I
920	939 w	–	939 w	γCH II
874	882 w	865 w	877 w	γCH I
856	865 w	–		γCH II
822	839 w	836 w	836 w	γCH I
798	–	–		γCH II
786	–	–	780 vw	γCH I
777	750 vvs	750 vw	736 sh	γCH I
711	731 vs	709 s	725 m	γCH II
691	689 s	686 sh	703 wsh	γPh I
680	663 m	663 w		υC–S
624	–	–		δPh I
614	613 w	–		δPh(X) II
597	–	601 vw		γPh(X) I
597	596 w	596 w	588 vw	γPh(X) II
521	515 w	–		γPh(X) I
518	508 w	507 w	509 s	γPh(X) II
493	–	–		δPh(X) II
483	477 w	462 w	462 w	δPh(X) II
449	458 w	–		γPh II
427	434 m	–	416 vw	γPh I
384	419 m	–		δPh(X) I
383	–	375 m	360 w	δPh(X) II
300	–	–		γPh(X) I, δPh(X) II
296	–	291 vw		γPh(X) II
216	–	233 w		δPh(X) I, II
			237 vvs	υAg–O
193	–	213 w		γPh(X) II
129	–	134 sh	158 s	γPh(X) I
118	–	96 s		tCH$_2$

υ, stretching; δ, in-plane bending; γ, out-of-plane deformation; ρ, rocking; t, torsional; ω, wagging; s, strong; w, weak; m, medium; v, very; br, broad; I, mono-substituted phenyl ring; II, disubstituted phenyl ring; X, substitutent sensitive; Ph, phenyl ring; subscript: as, asymmetric; s, symmetric.

1485 cm^{-1} (HF) are assigned as the scissoring mode of CH$_2$. Bands of hydrocarbons due to CH$_2$ twisting and wagging vibrations, are observed in the region 1180–1390 cm^{-1} [45,50]. These bands are generally appreciably weaker than those resulting from CH$_2$ scissoring vibrations. The CH$_2$ wagging and twisting modes are assigned at 1357 cm^{-1} (IR), 1347 cm^{-1} (Raman), 1372 cm^{-1} (HF) and 1214 cm^{-1} (HF), respectively. The band calculated at 1007 cm^{-1} is assigned as the rocking mode ρCH$_2$. The CO stretching vibration [49] absorbs moderately to strongly in the range 1045 ± 45 cm^{-1} and the band calculated at 1024 cm^{-1} is assigned as C$_{14}$–O$_{17}$ stretching mode.

Since the identification of all the normal modes of vibration of large molecules is not trivial, we tried to simplify the problem by considering each molecule as a substituted benzene. Such an idea has already been successfully utilized by several workers for the vibrational assignments of molecules containing multiple homo- and heteroaromatic rings [51–55]. In the following discussion, the mono-substituted and disubstituted phenyl rings are designated as rings I and II, respectively. The modes in the two phenyl rings will differ in wavenumber and the magnitude of splitting will depend on the strength of interactions between different parts (internal coordinates) of the two rings. For some modes, this splitting is so small that they may be considered as quasi-degenerate and for the other modes a significant amount of splitting is observed. Such observations have already been reported [51–53,56].

The existence of one or more aromatic rings in a structure is normally readily determined from the C–H and C≡C–C ring related vibrations. The C–H stretching occurs above 3000 cm^{-1} and is typically exhibited as a multiplicity of weak to moderate bands, compared with the aliphatic C–H stretch [57]. In the present case, the ab initio calculations give υC–H modes in the range of 2999–3037 cm^{-1}. The bands observed at 2985, 3029, 3052, 3088 cm^{-1} in the IR spectrum and at 2987, 3033, 3068, 3099 cm^{-1} in the Raman spectrum are assigned as the υC–H modes of the benzene ring.

The benzene ring possesses six ring stretching vibrations, of which the four with the highest wavenumbers (occurring respectively near 1600, 1580, 1490 and 1440 cm^{-1}) are good group vibrations. In the absence of ring conjugation, the band near 1580 cm^{-1} is usually weaker than that at 1600 cm^{-1}. The fifth ring stretching vibration is active near 1355 ± 35 cm^{-1}, a region which overlaps strongly with that of the CH in-plane deformation and the intensity is in general, low or medium [49,58]. The sixth ring stretching vibration or ring breathing mode appears as a weak band near 1000 cm^{-1} in mono-substituted benzenes [49]. The bands observed at 1601, 1587, 1559, 1522, 1454, 1436, 1315, 1278 cm^{-1} in the IR spectrum and at 1588, 1586, 1560, 1523, 1444, 1436, 1315, 1247 cm^{-1} in the Raman spectrum are assigned as υPh ring stretching modes. As seen from Table 2, the ab initio calculations give these modes [49] in the range 1612–1245 cm^{-1}.

The CH out-of-plane deformations [49] are observed between 1000 and 700 cm^{-1}. Generally, the C–H out-of-plane deformations with the highest wavenumbers have a weaker intensity than those at lower wavenumbers. The out-of-plane CH deformation at 750 cm^{-1} and the out-of-plane ring deformation at 689 cm^{-1} in the IR spectrum for a pair of strong bands characteristics of mono-substituted benzene derivative [49,59]. In the case of 1,2-disubstituted benzenes, a strong absorption in the region 755 ± 35 cm^{-1} is observed and is due to γCH, which is assigned at 731 cm^{-1} in the IR spectrum [51]. For benzothiazole derivatives [60] υC–S is reported at 648 cm^{-1} (Raman) and at 660 cm^{-1} (HF). In the present case the band at ∼663 cm^{-1} in both spectra is assigned as υC–S mode. Primary aromatic amines with nitrogen directly on the ring absorb strongly at 1330–1260 cm^{-1} due to stretching of the phenyl carbon–nitrogen bond [50]. Sandhyarani et al. [61] reported υCN at ∼1318 cm^{-1} for 2-mercaptobenzothiazole. For the title compound υC$_4$N$_{12}$ is observed at 1315 cm^{-1} in both spectra and the

Table 3
Calculated all β components and β_{tot} (×10^{-30} esu) values of the title compound.

β components	HF/6-31G*
β_{xxx}	−28.793
β_{xxy}	0.016
β_{xyy}	20.080
β_{yyy}	−0.015
β_{xxz}	6.310
β_{xyz}	0.010
β_{yyz}	22.979
β_{xzz}	50.614
β_{yzz}	−0.003
β_{zzz}	−4.608
β_{tot} (esu)	0.420 × 10^{-30}

calculated value is 1326 cm^{-1}. This mode is not pure but contains a significant contribution from the υPh mode.

5.2. Hyperpolarizability and geometrical parameters

Analysis of organic molecules having conjugated π-electron systems and large hyperpolarizability using infrared and Raman spectroscopy has evolved as a subject of research [62]. The potential application of the title compound in the field of nonlinear optics demands the investigation of its structural and bonding features contributing to the hyperpolarizability enhancement, by analyzing the vibrational modes using the IR and Raman spectra. The ring stretching bands at 1601, 1522, 1454, 1436 cm^{-1} observed in IR have their counterparts in Raman at 1588, 1523, 1444, 1436 cm^{-1}, respectively, and their relative intensities in IR and Raman spectra are comparable.

The first hyperpolarizability (β_0) of this novel molecular system is calculated using HF/6-31G* basis set, based on the finite field approach. In the presence of an applied electric field, the energy of a system is a function of the electric field. First hyperpolarizability is a third rank tensor that can be described by a 3 × 3 × 3 matrix. The 27 components of the 3D matrix can be reduced to 10 components due to the Kleinman symmetry [63].

The components of β are defined as the coefficients in the Taylor series expansion of the energy in the external electric field. When the electric field is weak and homogeneous, this expansion becomes

$$E = E_0 - \sum_i \mu_i F^i - \frac{1}{2}\sum_{ij}\alpha_{ij}F^iF^j - \frac{1}{6}\sum_{ijk}\beta_{ijk}F^iF^jF^k$$
$$- \frac{1}{24}\sum_{ijkl}\gamma_{ijkl}F^iF^jF^kF^l + \dots$$

where E_0 is the energy of the unperturbed molecule, F^i is the field at the origin, μ_i, α_{ij}, β_{ijk} and γ_{ijkl} are the components of dipole moment, polarizability, the first hyper polarizabilities, and second hyperpolarizibilites, respectively. The calculated first hyperpolarizability of the title compound is 0.42 × 10^{-30} esu. We conclude that the title compound is an attractive object for future studies of nonlinear optical properties (Table 3).

To the best of our knowledge, no X-ray crystallographic data of this molecule has yet been established. However, the theoretical results obtained are almost comparable with the recently reported structural parameters of the parent benzothiazole molecule [64]. From Table 1, it is clearly seen that the dihedral angles C$_6$–C$_5$–C$_4$–N$_{12}$ and C$_4$–N$_{12}$–C$_{13}$–C$_{14}$ are 180°. This indicates that the benzene ring II and the thiazole ring moieties of the title compound are planar as in the case of 2-amino-6-methylbenzothiazole [65]. For 2-amino-6-methylbenzothiazole [65] the bond lengths C$_4$–C$_5$, C$_4$–C$_3$, C$_3$–C$_2$, C$_4$–N$_{12}$, C$_{13}$–S$_{11}$, C$_3$–S$_{11}$ are respectively,
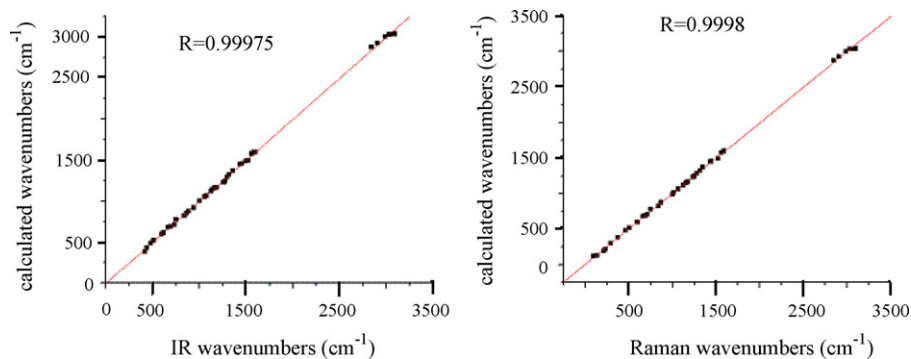
Fig. 5. Correlation graph.

1.4145, 1.4333, 1.4066, 1.4110, 1.3167, 1.8807, 1.8316 Å (DFT calculations). The corresponding values for the title compound are 1.3888, 1.3921, 1.3851, 1.4011, 1.2704, 1.8181 and 1.8095 Å. The ab initio calculations give the bond angles C_3–C_4–N_{12}, C_4–N_{12}–C_{13}, C_3–S_{11}–C_{13}, N_{12}–C_{13}–S_{11} as 114.9°, 113.3°, 86.7° and 115.4° for the title compound. These values are in agreement with the bond angles reported for 2-amino-6-methylbenzothiazole [65] (116.1°, 112.0°, 115.7°) and for 2-amino-4-methylbenzothiazole [60]. For 2-amino-4-methylbenzothiazole [60] the bond lengths C_3–C_4, C_3–S_{11}, C_{13}–N_{12}, C_4–N_{12} are 1.3916, 1.8046, 1.2962, 1.4173 Å, respectively and the bond angles C_5–C_4–C_3, C_4–C_3–S_{11}, C_3–S_{11}–C_{13}, are 120.2°, 108.8°, 88.1°, respectively.

In order to investigate the performance and vibrational wavenumbers of the title compound root mean square (RMS) and correlation coefficient between calculated and observed wavenumbers were calculated (Fig. 5). RMS values of wavenumbers were calculated using the following expression [66].

$$RMS = \sqrt{\frac{1}{n-1}\sum_{i}^{n}(\upsilon_i^{calc} - \upsilon_i^{exp})^2}$$

The RMS errors between the observed and scaled wavenumbers are found to be 18.52 and 18.35 for IR and Raman wavenumbers, respectively. Slight variation is found in the experimental and calculated vibrational modes. It must be due to the fact that hydrogen bond vibrations present in the crystal lead to strong perturbation of the infrared wavenumbers and intensities of many other modes. The experimental results belong to solid phase and theoretical calculations belong to gaseous phase.

5.3. SERS spectrum

SERS is already regarded as a valuable method because of its high sensitivity, which enables the detection and spectroscopic study of even single molecules [2]. The vibrational information contained in the SERS spectrum provide the molecular specificity required to characterize the adsorbate–surface interactions, specifically, the orientation of the adsorbed species on the metal surface. The relative intensities from the SERS spectra are expected to differ significantly from normal Raman spectra owing to specific surface selection rules [67]. The surface selection rule suggests that for a molecule adsorbed flat on the silver surface, its out-of-plane vibrational modes will be more enhanced when compared with its in-plane vibrational modes and vice versa when it is adsorbed perpendicular to the surface [67,68]. It is further seen that vibrations involving atoms that are close to the silver surface will be enhanced. When the wavenumber difference between Raman bands in normal and SERS spectra is not more than 5 cm^{-1}, the molecular plane is expected to be perpendicular to the silver surface [69].

In the SERS spectrum of the title compound, the aromatic C–H stretching vibration of ring I is observed as a strong band at 3060 cm^{-1} and as a weak band at 2994 cm^{-1}, which suggest that the phenyl ring I may be in a position close to the perpendicular orientation [69,70]. But for the phenyl ring II, the aromatic CH stretching vibrations are absent in the SERS spectrum, which means that the ring II may be somewhat flat on the silver surface [69,70].

It has also been documented in the literature [71] that when a benzene ring moiety interacts directly with a metal surface, the ring breathing mode is red shifted by 10 cm^{-1} along with substantial band broadening in the SERS spectrum. In the present case, the ring breathing mode of ring I is absent in the SERS spectrum while that of ring II is present at 1016 cm^{-1} without any wavenumber shift. Neither a substantial red shift nor significant band broadening was identified in the SERS spectrum of the title compound implying that the probability of a direct ring π-orbital to metal interaction should be low, in accordance to a tilted position of the ring.

The presence of CH$_2$ mode at 2953 cm^{-1} in the SERS spectrum indicates the closeness of CH$_2$ group with metal surface and interaction of the silver surface with phenoxy group. This is supported by the strong band at 237 cm^{-1} which may be due to Ag–O stretching vibration [72–74]. This band may be due to Ag–O/Ag–N/Ag–S stretching vibration. Apart from the interaction of the phenoxy group in the adsorption process, the fuzed thiazole moiety of the molecule can also bind to the silver surface through the lone pair of electrons of either the nitrogen or sulfur atoms or through both of them. A more favoured adsorption site can be enumerated theoretically by estimating the partial atomic charges on each of these probable active sites [75,76]. The higher the negative charge density on the atom the higher the probability of it acting as an adsorbative site for the silver substrate. Theoretical results estimated from HF ab initio calculations show that the partial atomic charges on the nitrogen, sulfur and oxygen atoms determined by natural population analysis are −0.514, 0.592 and −0.789, respectively. The negative charge density is thus observed to be more appreciable on the oxygen atom than others, thereby indicating the active involvement of the oxygen atom on the adsorption process. The appearance of a strong band at 237 cm^{-1} in the SERS spectrum ascribed to the Ag–O stretching indicates that the phenoxy group of the title compound is indeed adsorbed through the oxygen atom. The presence of a weak broad band at 1233 cm^{-1} due to υCO in the SERS spectrum supports the above argument.

The in-plane bending modes δCH of the aromatic ring are observed at 1172, 1066 cm^{-1} for ring I and 1120 cm^{-1} for ring II. The presence of these modes suggests that the benzene rings are oriented tilted to the silver surface [67,68]. Also the benzene ring vibrations observed at 1575, 1432 cm^{-1} (ring II), 1554, 1319 cm^{-1} (ring I) in the SERS spectrum supports this fact. According to the surface selection rules [77,78] the presence of in-plane vibrational modes at 1120, 462, 360 cm^{-1} (ring II), 1172, 1066 cm^{-1} (ring I) and

of the out-of-plane vibrational modes at 939, 588, 509 cm^{-1} (ring II), 996, 877, 836, 780, 736, 703, 416, 158 cm^{-1} (ring I) in the SERS spectrum of the title compound suggest that there is a certain angle between the rings and the surface of the silver particle. The substitute sensitive in-plane and out-of-plane bending modes are also detected at the same time, suggesting a tilted orientation of the molecule [79,80].

The charge transfer mechanism of SERS can be explained by the resonant Raman mechanism in which charge transfer excitation from the metal to the adsorbed molecule or vice versa occurs at the energy of the incident laser wavenumber [81,82]. The frontier orbital theory plays a significant role in the understanding of the charge transfer mechanism of SERS [83,84]. Two types of charge transfer mechanisms are predicted. One is molecule to metal and the other is metal to molecule. Molecule to metal charge transfer excitation occurs when an electron is transferred from the highest occupied molecular orbital (HOMO) of the adsorbate to the Fermi level of the metal. Conversely, transfer of an electron from the Fermi level of the metal to the lowest unoccupied molecular orbital (LUMO) results in metal to molecule charge transfer [60,83,85,86]. The theoretical results show that the HOMO, LUMO and LUMO +1 energies of the molecule are −0.308, −0.184 and −0.168 eV, respectively which are energetically much lower than the Fermi level of silver ($\sim$ +5.48 eV) [87]. Hence, we conclude that metal to molecule charge transfer interaction is more preferred here. The electron is probably transferred from metal to the LUMO of the molecule.

6. Conclusion

The FT-IR, FT-Raman and SERS spectra of 2-phenoxymethylbenzothiazole were studied. The molecular geometry and wavenumbers were calculated using the Hartree–Fock method with 6-31G* basis set. The observed wavenumbers were found to be in agreement with the calculated values. Optimized geometrical parameters of the title compound are in agreement with the reported values. It may be inferred that for 2-phenoxymethylbenzothiazole adsorbed on silver colloid, the molecule is adsorbed through the oxygen atom with the molecular plane tilted on the metal surface. Analysis of the phenyl ring modes shows that the C–C stretching mode is equally active as strong bands in both IR and Raman spectra, and is responsible for hyperpolarizability enhancement leading to nonlinear optical activity.

References

[1] R.C. Maher, L.F. Cohen, P. Etchegoin, Chem. Phys. Lett. 352 (2002) 378.
[2] S. Nie, S.R. Emory, Science 275 (1997) 1102.
[3] J. Bukowska, J. Mol. Struct. 275 (1992) 151.
[4] J. Chowdhury, M. Ghosh, T.N. Misra, J. Colloid Interface Sci. 228 (2000) 372.
[5] H.W. He, L.P. Mens, L.M. Hu, Z.J. Liu, Chin. J. Pestic. Sci. 4 (2002) 14.
[6] R.C. Elderfield, Heterocyclic Compounds, vol. 5, John Wiley and Sons, Inc., New York/London, 1956, p. 487.
[7] J.V.N. Vara-Prasad, A. Panapoulous, J.R. Rubin, Tetrahedron Lett. 41 (2000) 4065.
[8] E.G. Witte, H. Philipp, H. Vereecken, Org. Geochem. 29 (1998) 1829.
[9] R. Kloskowski, F. Fuhr, J. Environ. Sci. Health 22B (1987) 623.
[10] J.L. Bennet, D.P. Thomas, Mode of action of antitrematodal agents, in: W.C. Campbell, R.S. Rew (Eds.), Chemotherapy of Parasitic Disease, Plenum Press, New York, 1986, p. 427.
[11] R.O. McCracken, K.B. Lipkowitz, J. Parasitol. 76 (1990) 180.
[12] R.O. McCracken, K.B. Lipkowitz, J. Parasitol. 76 (1990) 853.
[13] M.Y. Yousef, A.M. Eisa, M.N. Nasra, S.A. El-Bialy, Mansoura J. Pharm. Sci. 13 (1997) 79.
[14] F. Delmas, A. Avellaneda, C.D. Giorgio, M. Robin, E. DeClercq, P. Timon-David, J.P. Galy, Eur. J. Med. Chem. 39 (2004) 685.
[15] I.H. Hall, N.J. Peaty, J.R. Henry, J. Easmon, G. Heinisch, G. Purstinger, Arch. Pharm. 332 (1999) 115.
[16] I. Hutchinson, T.D. Bradshaw, C.S. Matthews, M.F.G. Stevens, A.D. Westwell, Bioorg. Med. Chem. Lett. 13 (2003) 471.
[17] P.J. Palmer, R.B. Trigg, J.V. Warrington, J. Med. Chem. 14 (1971) 248.
[18] A. Benazzouz, T. Boraud, P. Dubedat, A. Boireau, J.M. Stutzmann, C. Gross, Eur. J. Pharmacol. 284 (1995) 299.

[19] B. Lara, L. Gandia, A. Torres, R. Martinez-Sierra, A.G. Garcia, M.G. Lopez, Eur. J. Pharmacol. 325 (1997) 109.
[20] T. Kotani, Y. Nagaki, A. Ishii, Y. Konishi, H. Tago, S. Suehiro, N. Okukado, K. Okamoto, J. Med. Chem. 40 (1997) 684.
[21] G. Sato, T. Chimoto, T. Aoki, S. Hosokawa, S. Sumigama, K. Tsukidate, F. Sagami, J. Toxicol. Sci. 24 (1999) 165.
[22] K. Oketani, T. Inoue, M. Murakami, Eur. J. Pharmacol. 427 (2001) 159.
[23] R. Paramashivappa, P.P. Kumar, P.V. SubbaRao, A. Srinivasa Rao, Bioorg. Med. Chem. Lett. 13 (2003) 657.
[24] A.A. Nagel, D.R. Liston, S. Jung, M. Mahar, L.A. Vincent, D. Chapin, Y.L. Chen, S. Hubbard, J.L. Ives, J. Med. Chem. 38 (1995) 1084.
[25] J.H. Matthews, R. Krishnan, M.J. Costanzo, B.E. Maryanoff, A. Tulinsky, Biophys. J. 71 (1996) 2830.
[26] R.G. Caccese, J.F. DiJoseph, J.S. Skotnicki, L.E. Borella, L.M. Adams, Agents Actions 34 (1991) 223.
[27] S.K. Sohn, M.S. Chang, W.S. Choi, K.B. Kim, T.W. Woo, S.B. Lee, Y.K. Chung, Can. J. Physiol. Pharmacol. 77 (1999) 330.
[28] M.F. Surgue, P. Gautheron, C. Schmitt, M.P. Viader, P. Conquet, R.L. Smith, N.N. Share, C.A. Stone, J. Pharmacol. Exp. Ther. 232 (1985) 534.
[29] C.W. Phoon, P.Y. Ng, A.E. Ting, S.L. Yeo, M.M. Sim, Bioorg. Med. Chem. Lett. 11 (2001) 1647.
[30] D. Loos, E. Sidoova, V. Sutoris, Molecules 4 (1999) 81.
[31] S.K. Ivanov, V.S. Yuritsyn, Neftekhimiya 11 (1971) 99;
     S.K. Ivanov, V.S. Yuritsyn, Chem. Abstr. 74 (1971) 12287m.
[32] MonsantoCo, Brit. Pat. 1,106,577 (1968);
     MonsantoCo, Chem. Abstr. 68 (1968) 96660t.
[33] A. Samat, R. Guglielmetti, J. Metzger, Helv. Chim. Acta 55 (1972) 1783.
[34] I. Yildiz-Oren, I. Yalcin, E. Aki-Sener, N. Ucarturk, Eur. J. Med. Chem. 39 (2004) 291.
[35] A. Pinar, P. Yurdakul, I. Yildiz, O.T. Arpaci, N.L. Acan, E.A. Sener, I. Yalcin, Biochem. Biophys. Res. Commun. 317 (2004) 670.
[36] P.C. Lee, D.J. Meisel, J. Phys. Chem. 86 (1982) 3391.
[37] H.I.S. Nogueira, Spectrochim. Acta 54A (1998) 1461.
[38] J.M. Aizpurua, C. Palomo, Soc. Chim. Fr. Bull. 15 (1984) 142.
[39] K.J. Frisch, G.W. Trucks, H.B. Schlegel, G.E. Scuseria, M.A. Robb, J.R. Cheeseman, J.A. Montgomery Jr., T. Vreven, K.N. Kudin, J.C. Burant, J.M. Millam, S.S. Iyengar, J. Tomasi, V. Barone, B. Mennucci, M. Cossi, G. Scalmani, N. Rega, G.A. Peterson, H. Nakatsuji, M. Hada, M. Ehara, K. Toyota, R. Fukuda, J. Hasegawa, M. Ishida, T. Nakajima, Y. Honda, O. Kitao, H. Nakai, M. Klene, X.J. Li, E. Knox, H.P. Hratchian, J.B. Cross, C. Adamo, J. Jaramillo, R. Gomperts, R.E. Stratmann, O. Yazyev, A.J. Austin, R. Cammi, C. Pomelli, J.W. Ochterski, P.Y. Ayala, K. Morokuma, G.A. Voth, P. Salvador, J.J. Dannenberg, V.G. Zakrzewski, S. Dapprich, A.D. Daniels, M.C. Strain, O. Farkas, D.K. Malick, A.D. Rabuck, K. Raghavachari, J.B. Foresman, J.V. Ortiz, Q. Cui, A.G. Baboul, S. Clifford, J. Cioslowski, B.B. Stefanov, G. Liu, A. Liashenko, P. Piskorz, I. Komaromi, R.L. Martin, D.J. Fox, T. Keith, M.A. Al-Laham, C.Y. Peng, A. Nanayakkara, M. Challacombe, P.M.W. Gill, B. Johnson, W. Chen, M.W. Wong, C. Gonzalez, J.A. Pople, Gaussian03, Revision C. 02, Gaussian Inc., Wallingford, CT, 2004.
[40] J.B. Foresman, in: E. Frisch (Ed.), Exploring Chemistry with Electronic Structure Methods, A Guide to Using Gaussian Inc., Pittsburg, PA, 1996.
[41] P. Flukiger, H.P. Luthi, S. Portmann, J. Weber, MOLEKEL 4. 3, Swiss Center for Scientific Computing, Manno, Switzerland, 2000–2002.
[42] S. Portmann, H.P. Luthi, Chimia 54 (2000) 766.
[43] I. Yalcin, E. Sener, T. Ozden, A. Akin, Eur. J. Med. Chem. 25 (1990) 705.
[44] R. Saxena, L.D. Kandpal, G.N. Mathur, J. Polym. Sci. A: Polym. Chem. 40 (2002) 3959.
[45] R.M. Silverstein, G.C. Bassler, T.C. Morril, Spectrometric Identification of Organic Compounds, 5th ed., John Wiley and Sons, Inc., Singapore, 1991.
[46] K. Nakamoto, Infrared and Raman spectrum of Inorganic and Coordination Compounds, 5th ed., John Wiley and Sons Inc., New York, 1997.
[47] T.D. Klots, W.B. Collier, Spectrochim. Acta 51A (1995) 1291.
[48] G. Yang, S. Matsuzono, E. Koyama, H. Tokuhisa, K. Hiratani, Macromolecules 34 (2001) 6545.
[49] N.P.G. Roeges, A Guide to the Complete Interpretation of Infrared Spectra of Organic Structures, John Wiley and Sons Inc., New York, 1994.
[50] N.B. Colthup, L.H. Daly, S.E. Wiberly, Introduction to Infrared and Raman Spectroscopy, 2nd ed., Academic Press, New York, 1975.
[51] P. Sett, N. Paul, S. Chattopadhyay, P.K. Mallick, J. Raman Spectrosc. 30 (1999) 277.
[52] P. Sett, N. Paul, S. Chattopadhyay, P.K. Mallick, Spectrochim. Acta 56A (2000) 855.
[53] P. Sett, S. Chattopadhyay, P.K. Mallick, J. Raman Spectrosc. 31 (2000) 177.
[54] V. Volovsek, G. Baranovic, L. Colombo, J.R. Durig, J. Raman Spectrosc. 22 (1991) 35.
[55] M. Muniz-Miranda, E. Castellucci, N. Neto, G. Sbrana, Spectrochim. Acta 39A (1983) 107.
[56] J.H.S. Green, Spectrochim. Acta 24 (1968) 1627.
[57] J. Coates, in: R.A. Meyers (Ed.), Interpretation of Infrared Spectra, A Practical Approach, John Wiley and Sons Inc., Chichester, 2000.
[58] G. Varsanyi, Assignments of Vibrational Spectra of Seven Hundred Benzene Derivatives, John Wiley and Sons Inc., New York, 1974.
[59] S. Higuchi, H. Tsuyama, S. Tanaka, H. Kamada, Spectrochim. Acta 30A (1974) 463.
[60] J. Sarkar, J. Chowdhury, M. Ghosh, R. De, G.B. Talapatra, J. Phys. Chem. 109B (2005) 22536.
[61] N. Sandhyarani, G. Skanth, S. Berchmanns, V. Yegnaraman, T. Pradeep, J. Colloid Interface Sci. 209 (1999) 154.

[62] M. Tommasini, C. Castiglioni, M. Del Zoppo, G. Zerbi, J. Mol. Struct. 480 (1999) 179.
[63] D.A. Kleinman, Phys. Rev. 126 (1962) 1977.
[64] A.A. El-Azhary, Spectrochim. Acta 55A (1999) 2437.
[65] J. Chowdhury, J. Sarkar, R. De, M. Ghosh, G.B. Talapatra, Chem. Phys. 330 (2006) 172.
[66] V. Krishnakumar, S. Dheivamalar, R.J. Xavier, V. Balachandran, Spectrochim. Acta 65A (2006) 147.
[67] J.A. Creighton, Spectroscopy of Surfaces—Advances in Spectroscopy, vol. 16, John Wiley and Sons Inc., New York, 1988 (p. 37, chapter 2).
[68] X. Gao, J.P. Davies, M.J. Weaver, J. Phys. Chem. A 94 (1990) 6858.
[69] G. Levi, J. Patigny, J.P. Massault, J. Aubard, Thirteenth International Conference on Raman Spectroscopy, Wurzburg, 1992, p. 652.
[70] J.S. Suh, M. Moskovits, J. Am. Chem. Soc. 108 (1986) 4711.
[71] P. Cao, M.J. Weaver, J. Phys. Chem. A 93 (1989) 6205.
[72] S. Kai, W. Chaozhi, X. Guangzhi, Spectrochim. Acta 45A (1989) 1029.
[73] C.Y. Panicker, H.T. Varghese, D. Philip, H.I.S. Nouguiera, Spectrochim. Acta 64A (2006) 744.
[74] S.J. Greaves, W.P. Griffith, J. Raman Spectrosc. 19 (1988) 503.
[75] J. Chowdhury, M. Ghosh, T.N. Misra, Spectrochim. Acta 56A (2000) 2107.
[76] J. Chowdhury, K.M. Mukherjee, T.N. Misra, J. Raman Spectrosc. 31 (2000) 427.
[77] M. Moskovits, J.S. Suh, J. Phys. Chem. 88 (1984) 5526.
[78] M. Moskovits, J.S. Suh, J. Phys. Chem. 92 (1988) 6327.
[79] D. Philip, A. John, C.Y. Panicker, H.T. Varghese, Spectrochim. Acta 57A (2001) 1561.
[80] K. Eckhard, J.K. Bert, J.M. Robert, J. Phys. Chem. 100 (1996) 5078.
[81] A. Campion, P. Kambhampati, Chem. Soc. Rev. 27 (1998) 241.
[82] J.F. Arenas, J. Soto, I. Lopez-Tocon, D.J. Fernandez, J.C. Otero, J.I. Marcos, J. Chem. Phys. 116 (2002) 7207.
[83] J. Sarkar, J. Chowdhury, P. Pal, G.B. Talapatra, Vib. Spectrosc. 41 (2006) 90.
[84] R.L. Garrell, J.E. Chadwick, D.L. Severance, N.A. McDonald, D.C. Myles, J. Am. Chem. Soc. 117 (1995) 11563.
[85] A.R. Bizzarri, S. Cannistraro, Chem. Phys. 290 (2003) 297.
[86] A.R. Bizzarri, S. Cannistraro, Chem. Phys. Lett. 395 (2004) 222.
[87] C. Kittel, Introduction to Solid State Physics, 5th ed., John Wiley and Sons Inc., New York, 1976, p. 154.